Androgen Levels Increase by Intratumoral *De novo* Steroidogenesis during Progression of Castration-Resistant Prostate Cancer

Jennifer A. Locke,[1] Emma S. Guns,[1] Amy A. Lubik,[1,2] Hans H. Adomat,[1] Stephen C. Hendy,[1] Catherine A. Wood,[1] Susan L. Ettinger,[1] Martin E. Gleave,[1] and Colleen C. Nelson[1,2]

[1]Department of Urologic Sciences, University of British Columbia, The Prostate Centre at Vancouver General Hospital, Vancouver, British Columbia, Canada; and [2]Institute of Health and Biomedical Innovation, Queensland University of Technology Brisbane, Australia

Abstract

Although systemic androgen deprivation prolongs life in advanced prostate cancer, remissions are temporary because patients almost uniformly progress to a state of a castration-resistant prostate cancer (CRPC) as indicated by recurring PSA. This complex process of progression does not seem to be stochastic as the timing and phenotype are highly predictable, including the observation that most androgen-regulated genes are reactivated despite castrate levels of serum androgens. Recent evidence indicates that intraprostatic levels of androgens remain moderately high following systemic androgen deprivation therapy, whereas the androgen receptor (AR) remains functional, and silencing the AR expression following castration suppresses tumor growth and blocks the expression of genes known to be regulated by androgens. From these observations, we hypothesized that CRPC progression is not independent of androgen-driven activity and that androgens may be synthesized *de novo* in CRPC tumors leading to AR activation. Using the LNCaP xenograft model, we showed that tumor androgens increase during CRPC progression in correlation to PSA up-regulation. We show here that all enzymes necessary for androgen synthesis are expressed in prostate cancer tumors and some seem to be up-regulated during CRPC progression. Using an *ex vivo* radiotracing assays coupled to high-performance liquid chromatography-radiometric/mass spectrometry detection, we show that tumor explants isolated from CRPC progression are capable of *de novo* conversion of [^{14}C]acetic acid to dihydrotestosterone and uptake of [^{3}H]progesterone allows detection of the production of six other steroids upstream of dihydrotestosterone. This evidence suggests that *de novo* androgen synthesis may be a driving mechanism leading to CRPC progression following castration. [Cancer Res 2008;68(15):6407–15]

Introduction

Within the prostate, androgens act to regulate gene networks that promote cell survival through the androgen receptor (AR), a ligand-responsive transcription factor. Androgen deprivation therapy (ADT) triggers apoptotic regression of both benign and malignant prostate epithelial cells. More than 80% of patients achieve symptomatic and objective responses following ADT and serum prostate-specific antigen (PSA) levels decrease in almost all patients (1). However, some cancer cells survive and proliferate in this androgen-depleted environment and consequently culminate in an "androgen-independent" or "castration-resistant" prostate cancer (CRPC) phenotype (2). Mechanisms underlying this tumor growth during CRPC have been attributed to a complex network of processes, including clonal selection (3), adaptive up-regulation of antiapoptotic and survival gene networks (4–6), cytoprotective chaperones (7, 8), and alternative mitogenic growth factor pathways (9–12). Almost uniformly, progression following an initial response to castration involves the reactivation of androgen-regulated processes, as illustrated by sentinel up-regulation of PSA, a discretely androgen-regulated gene (13). With the use of genome-wide expression profiling, evidence is mounting that in fact most androgen gene networks are reactivated in CRPC progression (14, 15). Two contending hypotheses stand to explain these observations: AR is aberrantly activated by signaling pathways or up-regulation of AR coactivators in the absence of androgens (16–18) or that androgen-regulated pathways within prostate cancer cells are activated by alternative sources of androgenic steroids (19–21).

Many reports address the former with a variety of suspect proteins and signaling pathways implicated (2, 22). The latter has also been investigated, primarily with the suggestion that adrenal androgens provide a systemic source of androgens to be used by prostate cancer tumors (20, 23). Mechanisms involving androgen production from an alternative source have been investigated in many trials evaluating maximal androgen blockade (MAB), which includes ketoconazole and/or antiandrogens, to block adrenal steroidogenesis in addition to medical or surgical castration (24). Results from these trials suggest that MAB leads to prolonged survival after 5 years but observed adverse side effects and decreased quality of life warrant further investigation of these secondary hormonal therapies (24, 25). Work in this area pioneered by Liu and colleagues and Labrie was reignited by Titus and colleagues who used liquid chromatography-mass spectrometry (LC-MS) to document levels of androgens, testosterone, and dihydrotestosterone in prostate tissues obtained from radical prostatectomy and recurrent prostate cancer patients who had "castrate" levels of serum androgens (26–28). We and others (14, 15, 29, 30) found that androgen-dependent genes become constitutively reexpressed in the absence of testicular androgens during CRPC progression and that down-regulation of AR expression following castration with small interfering RNA can suppress prostate cancer tumor growth (29, 30). Furthermore, many enzymes responsible for steroid synthesis have been observed to be up-regulated leading to the potential reactivation of AR (23).

Requests for reprints: Colleen Nelson, Department of Urologic Sciences, University of British Columbia, The Prostate Centre at Vancouver General Hospital, 2660 Oak Street, Vancouver, British Columbia, Canada V6H 3Z6. Phone: 604-875-4282; Fax: 604-875-5654; E-mail: colleen.nelson@ubc.ca.

doi:10.1158/0008-5472.CAN-07-5997

These data suggest that CRPC progression may not be entirely independent of androgen-driven activity of AR but, in fact, nontesticular sources of androgens are being capitalized on for AR activation. Furthermore, we hypothesize that androgens driving CRPC progression are synthesized *de novo* within the prostate cancer tumors and, in fact, may be increased by using a "feed forward" biosynthesis pathway as many of the enzymes are increased by androgens. In the prostate, androgens up-regulate the expression of sterol response element-binding protein (SREBP), a transcription factor that coordinately regulates cholesterol and fatty acid synthesis (15, 31). Androgens also stimulate the expression of Acyl-CoA–binding protein in prostate cells, which provides a rate-limiting step for steroidogenesis by facilitating the transport of cholesterol into the mitochondria for conversion to steroids (32). We have previously shown that the downstream genes coordinately regulated by SREBP are reactivated during disease progression (15); thus, *de novo* synthesis of steroids in prostate cancer cells may provide a plausible rationale for CRPC progression in the absence of testicular androgens.

Following these observations, we tested the hypothesis that this lipogenesis pathway beginning at acetic acid is converted to cholesterol and further metabolized to androgens in prostate tumor cells through a series of well-characterized stepwise enzymatic events. Androgen synthesis is often described in terms of the classic steroidogenic pathway through dehydroepiandrosterone and testosterone (Fig. 2); however, more recently, a "backdoor pathway" has been described as an alternative synthesis pathway that uses progesterone as the primary steroidal precursor of dihydrotestosterone, bypassing testosterone as an intermediate (33).

Following the establishment of LNCaP xenografts in intact male mice, mice were castrated and tumors were followed through CRPC progression as defined by the reexpression of PSA (34). In this report, we show that androgen levels within CRPC tumors are sufficient for AR activation, whereas corresponding serum androgens remain low in mice after castration (26–28). These tumors also produce relatively high concentrations of progesterone compared with downstream androgens, testosterone, and dihydrotestosterone. As adrenal cells are unable to synthesize progesterone without exogenous substrate addition (35) and these CPRC tumors express the necessary enzymes for progesterone and androgen synthesis at both the RNA and protein levels, we conducted further analytical assessments using metabolic radiotracing combined with tandem LC-MS and confirmed that CRPC tumors are indeed capable of *de novo* synthesis of androgenic steroids.

Materials and Methods

Materials. [1,2,4,5,6,7-^{3}H (N)]DHT (110.0 Ci/mmol; Perkin-Elmer Life Sciences, Inc.), [1,2,6,7-^{3}H (N)]progesterone (90.0Ci/mmol; Perkin-Elmer Life and Analytical Sciences), and [1(2)-^{14}C]acetic acid, sodium salt (55.0 mCi/mmol; Amersham Biosciences) were used for *in vitro* and *ex vivo* incubations and radiometric standards. Stock solutions of testosterone-16,16,17-d3 (deuterated testosterone; CDN Isotopes), 4-androstene-3,17-dione (Sigma), 4-pregnen-17-ol-3,20-dione (Steraloids, Inc.), 5α-androstan-17β-ol-3-one (Sigma), dihydrotestosterone (Sigma), 5β-pregnan-3α-27-diol-20-one (Steraloids), 5β-pregnan-3,20-dione (Steraloids), androsterone (Aldrich), cortisol (Sigma), pregnenolone (Sigma), progesterone (Sigma), R1881 (DuPont), and testosterone (Sigma) were prepared in 100% methanol as MS standards.

***In vitro* model: LNCaP cells.** LNCaP cells (passage 40–48; American Type Culture Collection) were cultured in RPMI 1640 (without phenol red) with L-glutamine, penicillin-streptomycin, and 5% charcoal-stripped serum (CSS; Hyclone).

***In vivo* model: LNCaP tumor progression to castrate resistance.** All animal experimentation was conducted in accord with accepted standards of the University of British Columbia Committee on Animal Care. LNCaP xenograft tumors were grown in athymic nude mice at four sites as modified from a previously reported method (15). PSA levels were measured by tail vein sera samples weekly using an immunoassay kit (ClinPro). At 6 wk after inoculation, mice were castrated. Tumors were harvested from the same mouse (39 mice total) before castration (PSA pre-Cx), 8 d after castration (PSA nadir), and 35 d after castration (PSA CRPC). Tumors were excised and dissected, and fragments were either immediately frozen in liquid nitrogen or placed in phenol red–free RPMI 1640 supplemented with 5% CSS.

Tumor homogenization. Frozen tumors were homogenized using a PowerGen 125 homogenizer for 35 s in buffer (20 mmol/L EDTA, 20 mmol/L NaCl, 20 mmol/L Tris) on ice. Internal standard (0.1 ng; deuterated testosterone) was added to each homogenate before extraction.

Steroid extraction. Supernatants, pellets, sera, and homogenates were extracted twice with ethyl acetate (1:1, v/v) and dried down using a CentriVap centrifugal evaporation system (35°C). Samples were then reconstituted in 100 μL of 50% methanol.

Steroid analysis by LC-MS. A Waters 2695 Separations Module coupled to a Waters Quattro Micro was used for LC-MS analysis. All MS data were collected in electrospray ionization positive (ESI+) mode with capillary voltage at 3 kV, source and desolvation temperatures of 120°C and 350°C, respectively, and N_2 gas flow of 450 L/h. Shorter chromatographic separations were carried out using a Waters Exterra 2.1 × 50 mm 3.5 μm, C18 column equilibrated with 20:80 acetonitrile (ACN):H_2O, ramped to 80:20 ACN:H_2O from 0.5 to 8.0 min, further to 95:5 from 8.0 to 9.0 min, and returned to 80:20 ACN:H_2O from 10.0 to 10.5 min with a total run time of 15 min. Flow rate was 0.3 mL/min, column temperature was 35°C, and 0.05% formic acid was present throughout the run. MS scan data for metabolite identification were collected using both 22 and 35 V for CV. Extracted ion chromatograms from extracted samples of radiolabeled alone (H) versus radiolabeled plus nonradiolabeled (cold) progesterone (H+C) spiked incubations were compared and LC retention time (RT) alignments were used to identify potential metabolites. Thus, precursor ions unique to the H+C sample fractions collected by high-performance liquid chromatography (HPLC) radiometric detection could be selected for further collision-induced dissociation (CID) at both 11 and 22 V CE for positive identification.

PCR and Western blot analysis of cells and tumors. Steroidogenic enzyme RNA quantification in tumor samples was assayed by quantitative reverse transcription-PCR (Q-RT-PCR) with the following primers: HSD3B2, 5′-cgggcccaactcctacaag-3′ (forward) and 5′-ttttccagaggctcttcttcgt-3′ (reverse); CYP17A1, 5′-gggcggcctcaaatgg-3′ (forward) and 5′-cagcgaaggcgaaggcgataccctta-3′ (reverse); CYP11A1, 5′-agttctcgggacttcgtcagt-3′ (forward) and 5′-ggagcccgccttcttga-3′ (reverse); HSD17B2, 5′-tttgccggagttttgaatgaa-3′ (forward) and 5′-gcaggttcttcgcaattcct-3′ (reverse); HSD17B3, 5′-tgggacagtgggcagtga-3′ (forward) and 5′-cgagtacgctttcccaattcc-3′ (reverse); HSD17B5, 5′-tgggaggccatggagaag-3′ (forward) and 5′-tttgacaccccaatggacttg-3′ (reverse); RDH5, 5′-gcccgccagcaatgc-3′ (forward) and 5′-cgcccaaagcctgagtca-3′ (reverse); SRD5A1, 5′-acgggcatcggtgcttaat-3′ (forward) and 5′-ccaacagtggcataggctttc-3′ (reverse); AKR1C2, 5′-gggaggccatggagaagtg-3′ (forward) and 5′-gttggacaccccgatgga-3′ (reverse); AKR1C1, 5′-ggaggccgtggagaagtgta-3′ (forward) and 5′-gttggacaccccgatgga-3′ (reverse); CYB5, 5′-cacccgcttcctcaacga-3′ (forward) and 5′-accagcttgttccagcagaac-3′ (reverse); and StAR, 5′-gcccatggagaggctctatg-3′ (forward) and 5′-ttccactcccccattgctt-3′ (reverse). Reactions were conducted with 0.4 μL of RT-PCR cDNA, 0.4 μL each of forward and reverse primers (10 μmol/L), 3.8 μL double-distilled water, and 5 μL Invitrogen Platinum SYBR Green qPCR Supermix-UDG with Rox. Triplicates of samples were run on the default settings of the ABI real-time PCR machine. Analysis was done using the SDS 2.1 program.

For Western blot analysis, tumor tissue was homogenized in radioimmunoprecipitation assay buffer [PBS, 1% Igepal (Sigma), 0.5% deoxycholate, 0.1% SDS, protease inhibitor mixture (Roche)], and protein

concentrations were assessed by the bicinchoninic acid method. Relative enzyme levels were quantified using the following antibodies at the indicated dilutions: rabbit polyclonal CYP17A1 (1:1,500) and rabbit polyclonal StAR (1:5,000) were both kindly donated by Dr. Hales (University of Illinois at Chicago, Chicago, IL; ref. 36); rabbit polyclonal CYP11A1 (1:1,500; Corgen, Inc.), goat monoclonal CYB5A (1:1,000; Abcam), goat polyclonal AKR1C3 (1:500; Abcam), and rabbit polyclonal HSD3B2 (1:20,000) were kindly donated by Dr. Thomas (University School of Medicine, Macon, GA); goat polyclonal SRD5A1 (1:1,000; Novus) and rabbit monoclonal HSD17B2 (1:500) kindly donated by Dr. Tremblay (Centre de Recherche de CHUL, Unite de Recherche en Ontogénie et Reproduction, Sainte-Foy, Quebec, Canada); mouse monoclonal HSD17B3 (1:250; Abnova); and mouse monoclonal RDH5 (1:250 Abnova).

***Ex vivo* [^{3}H]progesterone and [^{14}C]acetic acid treatment of cells and tumors.** Freshly excised tumor specimens were teased apart in 5 mL phenol red–free RPMI 1640 supplemented with 5% CSS. Excess debris and connective tissue were discarded and the remaining cells were centrifuged at 500 × *g* for 4 min. The supernatant was aspirated and the pellet was resuspended in fresh medium (2 mL per test condition) and transferred to six-well tissue culture plates. One hour after plating cells, either 0.001 mCi/mL [^{3}H]progesterone or 0.002 mCi/mL [^{14}C]acetic acid was added to the cultures. Samples for metabolite identification by MS received additional 10 μg/mL of unlabeled progesterone. After 4 d of incubation with radioisotope at 37°C and 5% CO_2, the cells were harvested and centrifuged at 13,500 × *g* for 10 min. The supernatant (medium) was transferred to a fresh tube and both cell pellet and supernatant were stored at −80°C.

HPLC separation and radiometric detection of ^{3}H- and ^{14}C-labeled steroids. A Waters 2695 Separations Module coupled with a Packard (Perkin-Elmer) Radiomatic Model 150TR detector equipped with a 0.5 mL flow cell provided chromatographic separation and detection of radiolabeled analytes. Separations of ^{3}H-labeled steroids were performed using a Waters Exterra 2.1 × 150 mm 5 μm, C18 column equilibrated with 10:90 ACN:H_2O, ramped to 25:75 ACN:H_2O (0.75–1.5 min), further to 35:65 ACN:H_2O (1.5–20 min), and then to 45:55 ACN:H_2O (25–30 min). Isopropanol (IPA) was introduced at this time from 45:0:55 ACN:IPA:H_2O to 45:55:0 ACN:IPA:H_2O (30–50 min), retained at 45:55:0 until 55 min, and returned to starting conditions at 57 min for reequilibration up to a 70-min run length. Separations of ^{14}C-labeled steroids were performed using the same C18 column equilibrated with 10:90 ACN:H_2O and ramped to 25:75 ACN:H_2O (0.75–1.5 min) and further to 60:40 ACN:H_2O (1.5–45 min). IPA was introduced at this time from 60:0:40 ACN:IPA:H_2O to 70:30:0 ACN:IPA:H_2O (45–50 min), retained at 60:40:0 until 60 min, and returned to starting conditions at 62 min for reequilibration up to a 70-min run length. LC flow rate was 0.3 mL/min, column temperature was 30°C, and Radiomatic scintillation fluid (Ultima-Flo M, Perkin-Elmer) flow rate was 1 mL/min. [^{3}H]dihydrotestosterone and [^{3}H]progesterone were used as RT standards. Radiometric RTs were observed to lag MS RT by ~1 min and this normalization factor was applied for the additional nonlabeled standards. For metabolite identification, [^{3}H]progesterone radiolabeled (H) versus radiolabeled plus nonradiolabeled (cold) progesterone (H+C) treated extracts were fractionated using the above LC method by setting the splitter of the Radiomatic detector to 20% with the remaining 80% of LC flow being collected in 1-min fractions and dried by centrifugal evaporation (CentriVap, 40°C for 3 h), and selected fractions were reconstituted in 100 μL of 50% methanol for subsequent MS analysis (above).

Results

Steroid levels are increased in LNCaP xenografts obtained from mice exhibiting CRPC progression but remain low in corresponding serum. Progesterone, testosterone, and dihydrotestosterone were quantified in LNCaP xenograft tissues obtained from the same mouse (n = 5) before castration (pre-Cx), 7 days after castration (N), and 28 days after castration (CRPC) when PSA is reexpressed and defines CRPC gene expression in this model. Both testosterone and dihydrotestosterone tissue levels seem to be elevated in CRPC tumors compared with N (Fig. 1*A*). In fact, tumor testosterone levels significantly decrease after castration (P = 0.007; 3.5% of pre-Cx) and then increase slightly once CRPC progression is reached as defined by PSA (20.2% of pre-Cx). Dihydrotestosterone concentrations as low as ~10^{-14} mol/L (2.92×10^{-6} ng/g) have been shown to transactivate AR in prostate cancer cell lines (37), and therefore, the levels observed in CPRC xenograft tumors ~6.5×10^{-10} mol/L (0.19 ± 0.07 ng/g tissue) would seem sufficient for AR activation (28). In agreement with previous studies (38), serum testosterone and dihydrotestosterone concentrations remarkably decrease following castration and remained low (<14% and 12% of pre-Cx, respectively) in mice exhibiting CPRC progression (Fig. 1*B*). Tumor progesterone levels were initially quite high before castration (Fig. 1*A*) and seem to increase (201% of

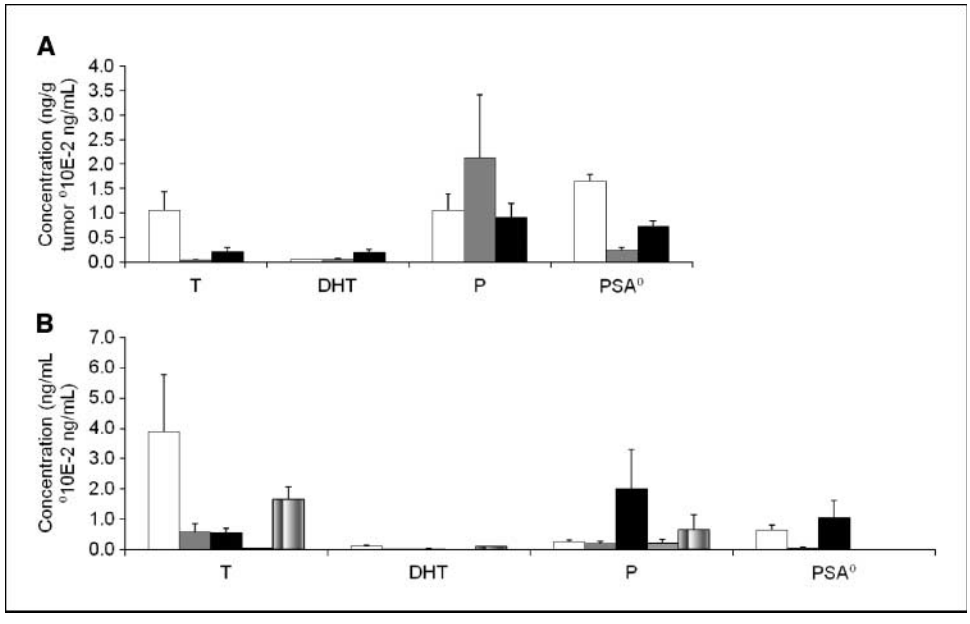

Figure 1. Mean concentrations of testosterone (*T*), dihydrotestosterone (*DHT*), and progesterone (*P*) in tumor homogenates obtained from mice before castration (pre-Cx; □, n = 5), 8 d after castration (N; ▩, n = 5), and 35 d after castration (CRPC; ■, n = 8). *A,* serum PSA was also monitored at time points indicated. *B,* mean concentrations of testosterone, dihydrotestosterone, progesterone, and PSA in serum samples obtained from pre-Cx (□, n = 5), N (▩, n = 5), CRPC (■, n = 5), castrate (non–tumor-bearing mouse; ▩, n = 3), and intact (non–tumor-bearing mouse; ▮, n = 3) mice. Testosterone, dihydrotestosterone, and progesterone concentrations (ng/g tumor + SE or ng/mL serum + SE) were normalized to internal standard (deuterated testosterone). PSA concentrations units were *10E−2 ng/mL. Statistically significant differences (P< 0.05) from AD and N groups are indicated by * and **, respectively.

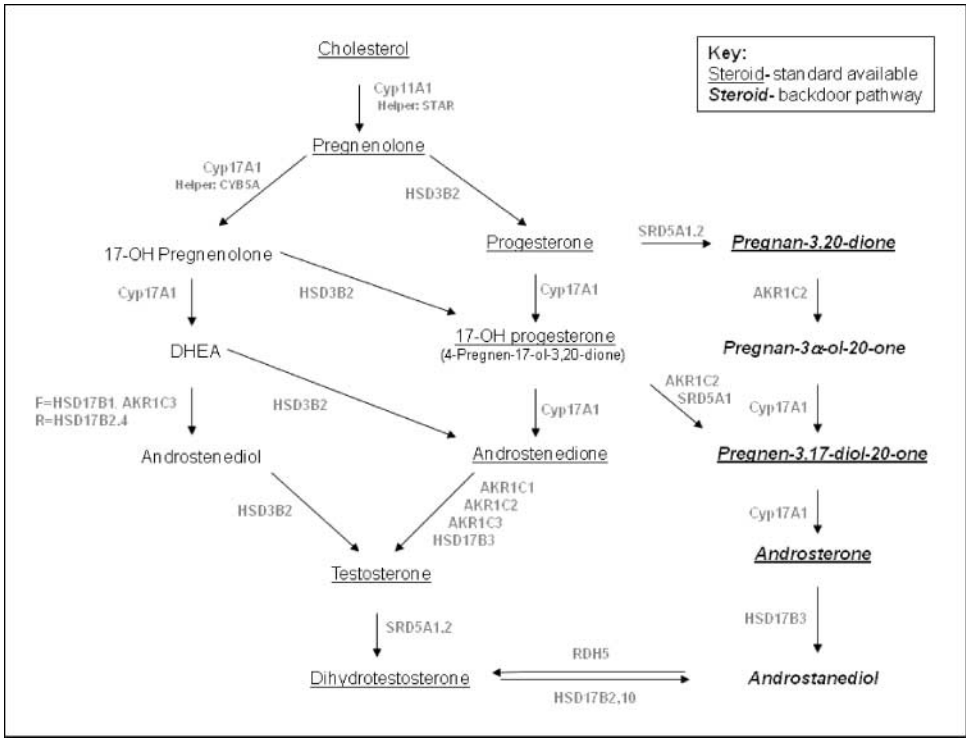

Figure 2. Schematic outline of the steroidogenic pathway from cholesterol to dihydrotestosterone, including the "backdoor" pathway (shown in *bold italics*; ref. 33). Standards were used for analysis of the underlined steroids.

pre-Cx) after castration. Furthermore, progesterone levels decrease to 86% of pre-castrate levels during CRPC progression. This trend opposing the characteristic PSA profile suggests that progesterone may be involved in an adaptation mechanism whereby the cancer cell initially adjusts to androgen deprivation by producing more androgen precursor, progesterone. Furthermore, serum progesterone is high (2.0 ± 1.3 ng/mL serum) in mice exhibiting CRPC progression, whereas serum progesterone from castrated non–tumor-bearing mice remains quite low (0.2 ± 0.1 ng/mL serum), suggesting that the tumor is the source of this progesterone surge (Fig. 1*B*). Progesterone, like dihydrotestosterone, is known to induce cholesterol synthesis in prostate cancer cells (39). It is therefore postulated that increased progesterone levels observed in tumors 7 days after castration and secreted in serum during CRPC progression may be significantly contributing to the underlying mechanisms of progression beyond cholesterol as an intermediate in androgen synthesis. In addition, we determined that the adrenal glands from mice exhibiting CRPC progression did not contain testosterone, dihydrotestosterone, or any of their steroid precursors at detectable levels by HPLC-MS/MS (data not shown) and thus do not seem to be the source of the observed dihydrotestosterone synthesis within our model. This is consistent with other studies as anticipated (40, 41). Furthermore, as circulating serum testosterone and dihydrotestosterone concentrations remain low after castration, the source of the increased androgen levels observed in tumors during progression is most likely from the LNCaP tumor itself.

mRNA and protein of the enzymes required to synthesize dihydrotestosterone from cholesterol are detected in LNCaP xenograft tumor tissues. Using Q-RT-PCR, we have verified the presence of mRNA corresponding to each of the enzymes required for dihydrotestosterone synthesis from cholesterol (Fig. 2) in pre-Cx, N, and CRPC xenograft tumors (Fig. 3*A*). The expression of StAR, HSD3B2, and RDH5 at the mRNA level significantly decrease at N relative to pre-Cx (P = 0.005, 0.014, and 0.011, respectively), whereas SRD5A1 and RDH5 significantly increase at CRPC relative to N (P = 0.002 and 0.011, respectively). Several other trends appear in the data. For example, CYP11A1, CYP17A1, CYB5A1, AKR1C1, AKR1C2, AKR1C3, and HSD17B2 seem to increase at CRPC relative to N. However, these trends did not reach statistical significance due to the intermouse variability in absolute levels.

Western blot analysis verified that the enzymes necessary for the *de novo* synthesis of steroids from cholesterol are expressed in LNCaP xenografts (Fig. 3*B*). In this analysis, tumors from separate inoculation sites were surgically removed at pre-Cx, N, and CRPC stages from seven mice. Trends similar to the mRNA levels support an increase in protein levels of nearly all of the steroidogenic enzymes during transition to the CRPC state.

[^{14}C]acetic acid is converted to dihydrotestosterone in androgen-starved LNCaP cells and CRPC tumor cells. Initially, androgen-starved *in vitro* LNCaP cells were incubated with cholesterol precursor [^{14}C]acetic acid and *de novo* conversion profiles were characterized using HPLC-radiometric detection. In these androgen-starved conditions, LNCaP cells synthesized large quantities of hydrophobic molecules consistent with cholesterol and a range of lipids (RT = 45–70 min; 91.0% conversion) as well as further minor conversion into steroids: progesterone, 4-pregnen-17-ol-3,20-dione, and dihydrotestosterone (0.4%, 0.6%, and 1.8% conversion, respectively) as determined by RT agreement with MS standards (Fig. 4*A*). Following this experiment, mice (n = 3), each bearing three tumors, were serially excised at the time points of pre-Cx, N, and CRPC, disaggregated, and cultured *ex vivo* with [^{14}C]acetic acid. The majority of *de novo* synthesis activity in pre-Cx and N tumors (representative example Fig. 4*B*), like *in vitro* LNCaP cells, appears in later eluting cholesterol and lipid peaks (RT = 45–70 min; 84.7% and 92.8% conversion) and not in the steroid eluting region (12.0% and 3.2% conversion) from RT of 18 to 45 min. However, in CRPC tumors, *de novo* synthesis of more

hydrophilic species with shorter RTs, including steroids (54.0% conversion), was observed. In fact, overall CRPC tumors (n = 3) were capable of *de novo* synthesis of analytes with matching RTs to standards 4-pregnen-17-ol-3,20-dione, progesterone, and dihydrotestosterone (4.0%, 1.5%, and 8.3% conversion, respectively) by MS.

[^{3}H]progesterone is converted to steroid precursors of dihydrotestosterone in both the classic and backdoor pathways in CRPC tumor cells. As tumor progesterone levels seem high after castration and enzymes necessary for progesterone synthesis from cholesterol (CYP11A1and StAR) and metabolism (CYP17A1 and SRD5A1) seem to be increased in CRPC tumors, it was hypothesized that progesterone is an important mediator of *de novo* synthesis of dihydrotestosterone in prostate cancer progression. To investigate the pathway (backdoor or classic) whereby progesterone leads to dihydrotestosterone synthesis, androgen-starved LNCaP cells were incubated with [^{3}H]progesterone and *de novo* conversion profiles were obtained (data not shown). These cells were capable of *de novo* synthesis of analytes with matching RT to that of our testosterone, 4-pregnene-17-ol-3,20-dione, 5-pregnan-3,17-diol, androsterone, pregnan-3,20-dione, and dihydrotestosterone standards by MS. We further incubated excised CRPC tumors *ex vivo* with [^{3}H]progesterone in a time course experiment to explore the kinetics of this conversion to downstream steroids. Medium was sampled from radiolabeled tumors at 3, 18, 24, 48, and 96 h with corresponding radiometric LC profiles of extracts shown in Fig. 4*C*. Major steroid products are evident at 18, 21, 34, 36, 39, 41, and 44 min in addition to intact progesterone, which remained after 96 h. These data reflect a complex series of steroidogenic metabolic steps ongoing in this CRPC tumor model system over time.

To conclusively identify the *de novo* synthesized steroids in either the classic or backdoor pathway from [^{3}H]progesterone to dihydrotestosterone, extracts from supernatants of both [^{3}H]progesterone (H) and ^{3}H plus nonlabeled progesterone (H+C) treatment also underwent radiometric HPLC analysis (Fig. 4*D*) with a fraction diverted and collected for further MS analysis. Multiple reaction monitoring (MRM) analysis, ESI+ MS scans, and fragment ion scans using the masses selected from scan data were performed. Equivalent fractions from (H)- and (H+C)-labeled samples from the same tumor were compared to identify unique masses. Analysis of *ex vivo* cells from CRPC tumors incubated with (H+C) progesterone, illustrated steroids predominant in both the classic and backdoor pathways to dihydrotestosterone synthesis (pregnenolone, 4-pregnen-17-ol-3,20-dione, pregnan-3,20-dione, pregnen-3,17-diol-20-one, androsterone, and androstenedione) was identified and semiquantitatively assessed by MRM data using a two-point calibration versus standard. In addition, some peaks were evident with RT, which differed from those determined for known standards, representing different steroids with a common transition (Fig. 5). Precursor mass and fragmentation patterns for these unknowns are consistent with a steroidal entity; however, their precise identities are currently being investigated.

Discussion

Castrate-resistant disease is defined by rising PSA following ADT and by many lines of evidence suggests reactivation of the AR (13, 14). In attempting to account for this observation, some researchers hypothesize that adrenal androgens are synthesized during CRPC progression and supply the prostate tumors with androgen following ADT administered through either LHRH agonist action or physical castration (20, 23). Consequently, attempts have been made clinically to induce total suppression of androgen blockade using ketoconazole to block adrenal steroidogenesis and/or antiandrogens to directly antagonize the AR in addition to castration (24). However, the basic premise of this hypothesis has recently been met with skepticism. Research carried out by Liu and colleagues and Labrie, and more recently by Titus and colleagues, shows that substantial amounts of androgens, testosterone, and dihydrotestosterone are present in human

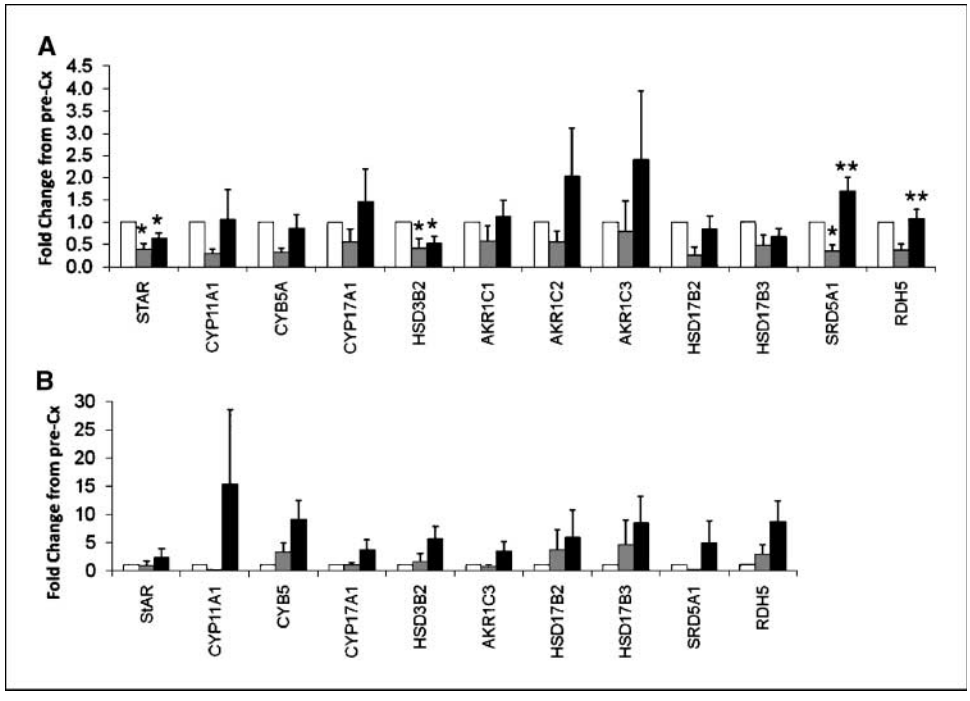

Figure 3. *A,* Q-RT-PCR analysis of twelve enzymes involved in the steroidogenic pathway in pre-Cx (□), N (▩), and CRPC (■) tumor homogenates taken from the same mouse (n = 7). *Columns,* mean fold change in fluorescence readings from pre-Cx group for each enzyme; *bars,* SE. Statistically significant differences (P < 0.05) from pre-Cx and N groups are indicated by * and **, respectively. *B,* protein analysis of the 10 indicated enzymes in pre-Cx, N, and CRPC tumors from each mouse (n = 7). Fluorescence and Western blot readings were normalized to PSA of each mouse at time of tumor excision. Sometimes, two tumors were taken from the same mouse at CRPC. Vinculin was used as a loading control.

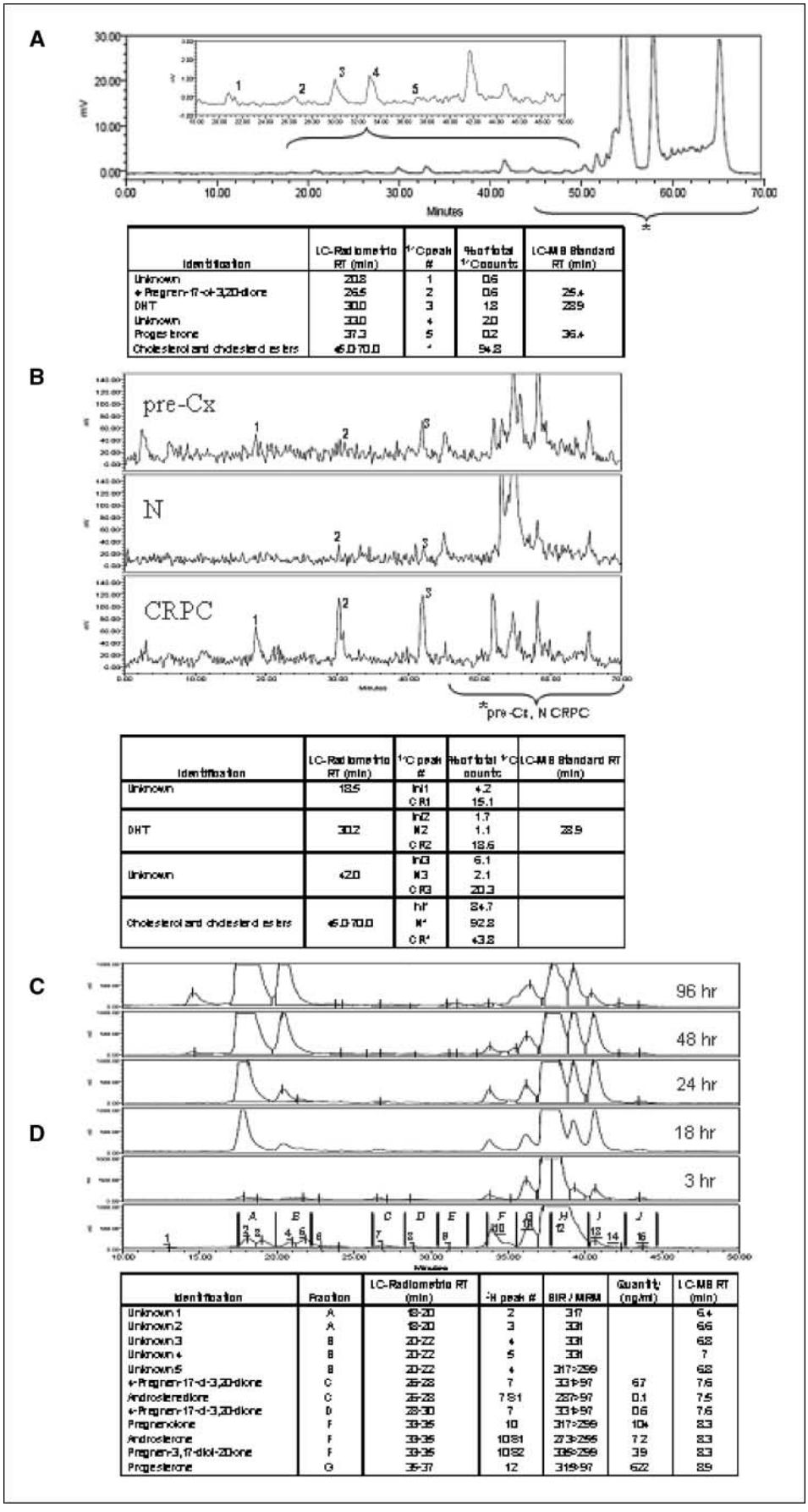

Identification	LC-Radiometric RT (min)	^{14}C peak #	% of total ^{14}C counts	LC-MS Standard RT (min)
Unknown	20.8	1	0.6	
4-Pregnen-17-ol-3,20-dione	26.5	2	0.6	25.4
DHT	30.0	3	1.8	28.9
Unknown	33.0	4	2.0	
Progesterone	37.3	5	0.2	36.4
Cholesterol and cholesterol esters	65.0-70.0	*	94.8	

Identification	LC-Radiometric RT (min)	^{14}C peak #	% of total ^{14}C counts	LC-MS Standard RT (min)
Unknown	18.5	IN1	4.2	
		C:R1	15.1	
DHT	30.2	IN2	1.7	28.9
		N2	1.1	
		C:R2	18.6	
Unknown	42.0	IN3	6.1	
		N3	2.1	
		C:R3	20.3	
Cholesterol and cholesterol esters	65.0-70.0	IN*	84.7	
		N*	92.8	
		C:R*	43.8	

Identification	Fraction	LC-Radiometric RT (min)	^{3}H peak #	SIR / MRM	Quantity (ng/mL)	LC-MS RT (min)
Unknown 1	A	18-20	2	317		6.4
Unknown 2	A	18-20	3	331		6.6
Unknown 3	B	20-22	4	331		6.8
Unknown 4	B	20-22	5	331		7
Unknown 5	B	20-22	4	317>259		6.8
4-Pregnen-17-ol-3,20-dione	C	26-28	7	331>97	67	7.6
Androstenedione	C	26-28	7 S1	287>97	0.1	7.5
4-Pregnen-17-ol-3,20-dione	D	28-30	7	331>97	0.6	7.6
Pregnenolone	F	33-35	10	317>259	10.4	8.3
Androsterone	F	33-35	10 S1	273>255	7.2	8.3
Pregnen-3,17-diol-20-one	F	33-35	10 S2	305>259	3.9	8.3
Progesterone	G	35-37	12	315>97	6.22	8.9

Figure 4. Example chromatographic analysis of extracted supernatants of *in vitro* ($n = 3$; *A*) and *ex vivo* pre-Cx ($n = 3$), N ($n = 3$), and CRPC ($n = 3$; *B*) LNCaP cells (from the same mouse) cultured in [^{14}C]acetic acid for 96 h *in vitro*. Identification of steroids in underlying LC radiometrically detected peaks (*in vitro* LNCaP, *1–5*; pre-Cx, N, and CRPC, *1–3*) by RT matchup to LC-MS standard analysis, along with % of total ^{14}C counts, is illustrated for *in vitro* and *ex vivo* chromatograms in *A* and *B*, respectively. Both the LC-radiometric and LC-MS runs are 70 min (~1 min lag time between LC-radiometric and LC-MS analysis). *C,* example chromatographic analysis of extracted supernatants of *ex vivo* CRPC LNCaP cells ($n = 3$) cultured in [^{3}H]progesterone for 3, 18, 24, 48, and 96 h *in vivo*. *D,* example chromatographic analysis of extracted supernatant from *ex vivo* CRPC LNCaP tumor cells ($n = 3$) cultured in ^{3}H + 10 μg/mL progesterone for 96 h *in vivo*. *C, 1* to *15,* peaks detected by radiometric detection; *A* to *J,* LC fractions collected for further LC-MS analysis. The LC-MS run is 15 min compared with the 70-min radiometric run. Correct combined MRM/RT variables are the basis for all identifications. S1 and S2 designations indicate presence of analyte in shoulder of peak. Quantitation is via two-point calibration. No steroids were observed in fractions E and J.

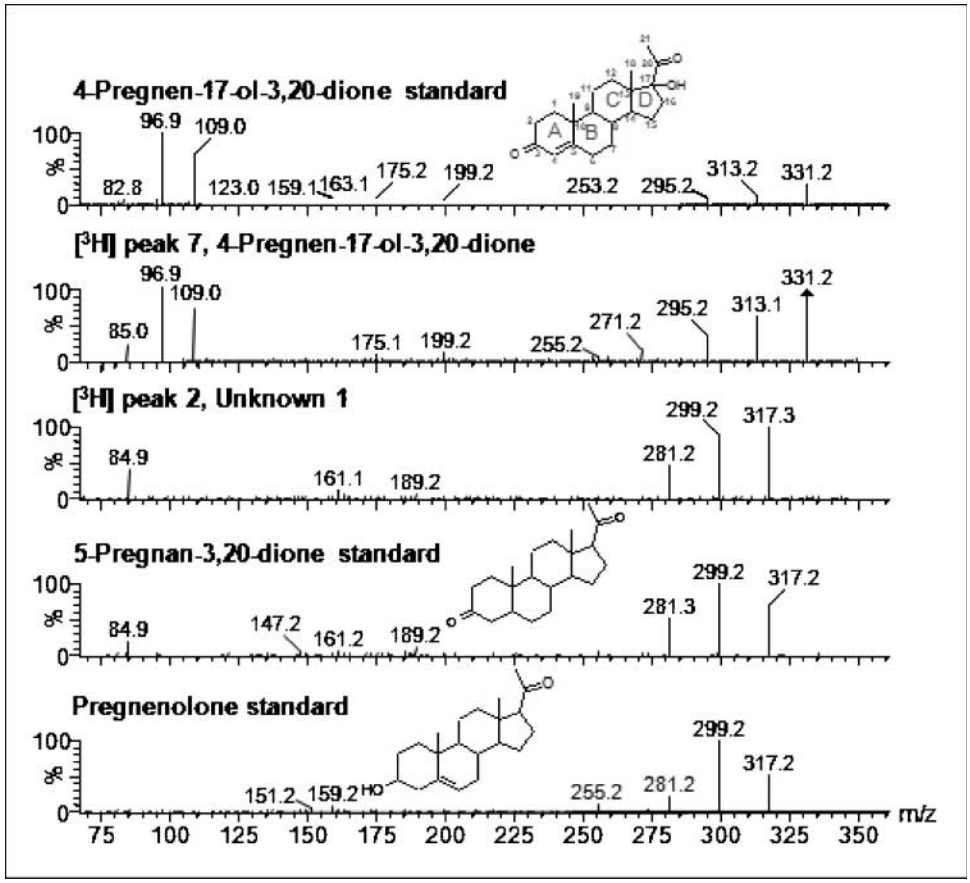

Figure 5. Fragment ion scans of positively identified steroid 4-pregnen-17-ol-3,20-dione (*peak 7*) as well as unknown 1 (*peak 2*) from the extract of the ^{3}H + 10 μg/mL progesterone-treated *ex vivo* LNCaP cells (n = 3) supernatant compared with steroids standards. Unknown 1 shows high similarity to 5-pregnan-3,20-dione and less to pregnenolone, however, RTs differ. Steroid structures are also depicted.

prostate tissues in levels capable of activation of AR despite castrate circulating androgen levels in serum (26–28). We show that CRPC tumors develop compensatory mechanisms during androgen deprivation, tailored to the synthesis of intratumoral androgens, triggering AR activation and disease progression. The increased testosterone and dihydrotestosterone levels observed in CRPC LNCaP tumors reinforce the observations in patients, with corresponding low-level circulating testosterone and dihydrotestosterone in sera. In addition, the reported intratumoral concentrations of testosterone and dihydrotestosterone seem to be sufficient for AR transactivation and the further observed induction of androgen-regulated genes (37). This suggests that androgens are not supplied via circulation from an external source such as the mouse adrenal glands (which were shown to lack steroid precursors of dihydrotestosterone as well; data not shown) to the prostate. Furthermore, using LC-MS, we show that tumor progesterone levels are high immediately after castration when circulating progesterone remains low. Therefore, we postulate that progesterone produced through extension of the cholesterol synthesis pathway may be crucial for the *de novo* synthesis of dihydrotestosterone within the local environment of the tumor. In keeping with this, in 2004, Payne and Hales (42) reviewed past studies investigating the *de novo* synthesis of hormones in diseased forms of cardiac tissues and nerves as a potential compensatory mechanism for cell survival.

We observed that LNCaP tumors contain all enzymes necessary for dihydrotestosterone synthesis. Furthermore, SRD5A1 and RDH5, enzymes responsible for progesterone metabolism to dihydrotestosterone via the backdoor pathway, were up-regulated in mRNA during transition to CRPC state as defined by reactivation of PSA. In agreement with Stanbrough and colleagues' findings (23), up-regulation of ARK1C1, AKR1C2, and AKR1C3 also appears during CRPC progression. We are, however, limited in our ability to determine statistically conclusive trends in enzyme expression at both the mRNA and protein level due to interanimal variability in time to progression observed in our xenograft mouse model. Nonetheless, the LNCaP tumors were confirmed to express steroidogenic enzymes with a trend of increase in CRPC and this was validated at both the mRNA and protein level.

We also show [^{14}C]acetic acid conversion to steroids and verify that CRPC tumors are capable of *de novo* androgen synthesis, albeit the downstream androgenic metabolites are detectable in moderate proportions. Acetic acid is a precursor to many molecules, including cholesterol, lipids (triacylglycerides and phospholipids), and fatty acids, and therefore a significant dilution of signal to steroids is expected (39). Furthermore, rate-limiting enzymatic reactions involving CYP11A1 and helper enzyme, StAR, recognized for their ability to shuttle cholesterol into the cell and convert it to upstream steroid pregnenolone, are known to regulate androgen biosynthesis (43, 44) and may be the rate-limiting enzymes in our acetic acid conversion to steroids. Previously, Acevedo and Goldzieher (45) also reported low conversion rates of steroidogenic metabolite precursors to androgens. Nonetheless, we have definitively shown conversion of [^{14}C]acetic acid to dihydrotestosterone in CRPC LNCaP xenograft cells using LC-radiometric detection. Testosterone did not seem to be synthesized in [^{14}C]acetic acid conversion assays, whereas the formation of two upstream steroids, progesterone and 4-pregnen-17-ol-3,20-dione, was observed. Lack of testosterone synthesis in tumor cells

suggests that the backdoor pathway to dihydrotestosterone may be used. Furthermore, mRNA up-regulation of backdoor pathway–specific enzyme, RDH5 alongside SRD5A1, an enzyme responsible for backdoor pathway entry from progesterone, was observed in CRPC tumors, thus further supporting the use of the backdoor pathway in CRPC progression.

We found progesterone to be a predominant steroid detected in significant quantities in pre-Cx, N, and CRPC LNCaP tumors and, as an upstream steroidogenic precursor to androgen via both the classic and backdoor pathways, we also incorporated progesterone into assays to determine metabolic activity in CRPC tumor cells. On MS/MS analysis of samples from HPLC-radiometric fractionation, the identities of most dihydrotestosterone precursors (with the exception of testosterone) in both the classic and backdoor pathways were confirmed as being synthesized in LNCaP cells and CRPC tumors. The lack of testosterone observed suggests that prostate cancer cells use the backdoor pathway to dihydrotestosterone synthesis and we further propose that this may result from inefficient CYP17A1 lyase activity as suggested by Auchus (33). Further investigations of this potential mechanism to backdoor synthesis of dihydrotestosterone as well as the identification of steroidal unknowns are currently under way. Our ability to identify steroids synthesized (as determined by MRMs) has been restricted by the availability of commercially available steroid standards. We understand that progesterone metabolite, unknown 1, has previously been documented but not identified in the literature (45) and is thought to be a hydroxylated steroid with a similar structure to pregnan-3,20-dione.

In summary, we report evidence that CRPC tumors (*a*) contain sufficient levels of testosterone and dihydrotestosterone for AR transactivation, (*b*) express all necessary enzymes for *de novo* synthesis of dihydrotestosterone, (*c*) are capable of intratumoral conversion of precursor [^{14}C]acetic acid to dihydrotestosterone, and (*d*) use progesterone to synthesize dihydrotestosterone through various steroid intermediates in both the classic and backdoor steroidogenic pathways.

This research attempts to provide rational explanation for consistent reports in the literature of the concerted up-regulation of androgen-regulated pathways characteristic of CRPC tissues as well as the presence of high tissue levels of androgens relative to low circulating androgen levels (14, 15, 46). CRPC progression remains a major obstacle to treatment of advanced prostate cancer. Improving our understanding of the underlying mechanisms of CRPC progression will provide a valuable insight for identifying new therapeutic targets and strategies.

Disclosure of Potential Conflicts of Interest

No potential conflicts of interest were disclosed.

Acknowledgments

Received 10/29/2007; revised 4/3/2008; accepted 4/24/2008.

Grant support: National Cancer Institute of Canada grants 012003 and 017007.

The costs of publication of this article were defrayed in part by the payment of page charges. This article must therefore be hereby marked *advertisement* in accordance with 18 U.S.C. Section 1734 solely to indicate this fact.

We thank John Cavanagh, Andy Eberding, Mary Bowden, and Rob Drapala for excellent technical support.

References

1. Goldenberg SL, Gleave ME, Taylor D, Bruchovsky N. Clinical experience with intermittent androgen suppression in prostate cancer: minimum of 3 years' follow-up. Mol Urol 1999;3:287–92.
2. Scher HI, Sawyers CL. Biology of progressive, castration-resistant prostate cancer: directed therapies targeting the androgen-receptor signaling axis. J Clin Oncol 2005;23:8253–61.
3. Isaacs JT. The biology of hormone refractory prostate cancer. why does it develop? Urol Clin North Am 1999; 26:263–73.
4. Gimenez-Bonafe P, Fedoruk MN, Whitmore TG, et al. YB-1 is upregulated during prostate cancer tumor progression and increases P-glycoprotein activity. Prostate 2004;59:337–49.
5. Fedoruk MN, Gimenez-Bonafe P, Guns ES, Mayer Lawrence D, Nelson CC. P-glycoprotein increases the efflux of the androgen dihydrotestosterone and reduces androgen responsive gene activity in prostate tumor cells. Prostate 2004;59:77–90.
6. Gleave M, Tolcher A, Miyake H, et al. Progression to androgen independence is delayed by adjuvant treatment with antisense bcl-2 oligodeoxynucleotides after castration in the LNCaP prostate tumor model. Clin Cancer Res 1999;5:2891–8.
7. Rocchi P, So A, Kojima S, et al. Heat shock protein 27 increases after androgen ablation and plays a cytoprotective role in hormone-refractory prostate cancer. Cancer Res 2004;64:6595–602.
8. Rocchi P, Beraldi E, Ettinger S, et al. Increased Hsp27 after androgen ablation facilitates androgen-independent progression in prostate cancer via signal transducers and activators of transcription 3-mediated suppression of apoptosis. Cancer Res 2005;65:11083–93.
9. Culig Z. Androgen receptor cross-talk with cell signaling pathways. Growth Factors 2004;22:179–84.
10. Craft N, Shostak Y, Carey M, Sawyers CL. A mechanism for hormone-independent prostate cancer through modulation of androgen receptor signaling by the HER-2/neu tyrosine kinase. Nat Med 1999;5:280–5.
11. Miyake H, Nelson C, Rennie PS, Gleave ME. Overexpression of insulin-like growth factor binding protein-5 helps accelerate progression to androgen-independence in the human prostate LNCaP tumor model through activation of phosphatidylinositol 3′-kinase pathway. Endocrinology 2000;141:2257–65.
12. So A, Gleave M, Hurtado-Col A, Nelson C. Mechanisms of the development of androgen independence in prostate cancer. World J Urol 2005;23:1–9.
13. Huang W, Shostak Y, Tarr P, Sawyers C, Carey M. Cooperative assembly of androgen receptor into a nucleoprotein complex that regulates the prostate-specific antigen enhancer. J Biol Chem 1999;274:25756–68.
14. Mostaghel EA, Page ST, Lin DW, et al. Intraprostatic androgens and androgen-regulated gene expression persist after testosterone suppression: therapeutic implications for castration-resistant prostate cancer. Cancer Res 2007;67:5033–41.
15. Ettinger SL, Sobel R, Whitmore TG, et al. Dysregulation of sterol response element-binding proteins and downstream effectors in prostate cancer during progression to androgen independence. Cancer Res 2004;64:2212–21.
16. Culig Z, Bartsch G. Androgen axis in prostate cancer. J Cell Biochem 2006;99:373–81.
17. Singh P, Uzgare A, Litvinov I, Denmeade SR, Isaacs JT. Combinatorial androgen receptor targeted therapy for prostate cancer. Endocr Relat Cancer 2006;13:653–66.
18. Chmelar R, Buchanan G, Need EF, Tilley W, Greenberg NM. Androgen receptor coregulators and their involvement in the development and progression of prostate cancer. Int J Cancer 2007;120:719–33.
19. Titus Mark A, Schell Michael J, Lih Fred B, Tomer Kenneth B, Mohler James L. Testosterone and dihydrotestosterone tissue levels in recurrent prostate cancer. Hum Cancer Biol 2005;11:4653–7.
20. Mohler JL, Gregory CW, Ford OH III, et al. The androgen axis in recurrent prostate cancer. Clin Cancer Res 2004;10:440–8.
21. Han G, Buchanan G, Ittmann M, et al. Mutation of the androgen receptor causes oncogenic transformation of the prostate. Proc Natl Acad Sci U S A 2005;102:1151–6.
22. Dehm SM, Tindall DJ. Molecular regulation of androgen action in prostate cancer. J Cell Biochem 2006;99:333–44.
23. Stanbrough M, Bubley GJ, Ross K, et al. Increased expression of genes converting adrenal androgens to testosterone in androgen-independent prostate cancer. Cancer Res 2006;66:2815–25.
24. Samson DJ, Seidenfeld J, Schmitt B, et al. Systematic review and meta-analysis of monotherapy compared with combined androgen blockade for patients with advanced prostate carcinoma. Cancer 2002;95:361–76.
25. Small EJ, Ryan CJ. The case for secondary hormonal therapies in the chemotherapy age. J Urol 2006; 176:S66–71.
26. Liu J, Geller J, Albert J, Kirshner M. Acute effects of testicular and adrenal cortical blockade on protein synthesis and dihydrotestosterone content of human prostate tissue. J Clin Endocrinol Metab 1985;61:129–33.
27. Labrie F. Adrenal androgens and intracrinology. Semin Reprod Med 2004;22:299–309.
28. Titus MA, Gregory CW, Ford OH III, Schell MJ, Maygarden SJ, Mohler JL. Steroid 5α-reductase isozymes I and II in recurrent prostate cancer. Clin Cancer Res 2005;11:4365–71.
29. Gregory CW, Hamil KG, Kim D, et al. Androgen receptor expression in androgen-independent prostate cancer is associated with increased expression of androgen-regulated genes. Cancer Res 1998;58:5718–24.
30. Chen CD, Welsbie DS, Tran C, et al. Molecular determinants of resistance to antiandrogen therapy. Nat Med 2004;10:33–9.
31. Swinnen JV, Heemers H, van de Sande T, et al. Androgens, lipogenesis and prostate cancer. J Steroid Biochem Mol Biol 2004;92:273–9.
32. Papadopoulos V, Amri H, Boujrad N, et al. Peripheral benzodiazepine receptor in cholesterol transport and steroidogenesis. Steroids 1997;62:21–8.

33. Auchus RJ. The backdoor pathway to dihydrotestosterone. Trends Endocrinol Metab 2004;15:432–8.

34. Gleave ME, Hsieh JT, Wu HC, von Eschenbach AC, Chung LW. Serum prostate specific antigen levels in mice bearing human prostate LNCaP tumors are determined by tumor volume and endocrine and growth factors. Cancer Res 1992;52:1598–605.

35. Yanase T, Gondo S, Okabe T, et al. Differentiation and regeneration of adrenal tissues: an initial step toward regeneration therapy for steroid insufficiency. Endocr J 2006;53:449–59.

36. Hales DB, Sha LL, Payne AH. Testosterone inhibits cAMP-induced *de novo* synthesis of Leydig cell cytochrome P-450(17α) by an androgen receptor-mediated mechanism. J Biol Chem 1987;262:11200–6.

37. Gregory CW, Johnson RT, Jr., Mohler JL, French FS, Wilson EM. Androgen receptor stabilization in recurrent prostate cancer is associated with hypersensitivity to low androgen. Cancer Res 2001;61:2892–8.

38. Kyprianou N, Isaacs JT. Biological significance of measurable androgen levels in the rat ventral prostate following castration. Prostate 1987;10:313–24.

39. Swinnen JV, Van Veldhoven PP, Esquenet M, Heyns W, Verhoeven G. Androgens markedly stimulate the accumulation of neutral lipids in the human prostatic adenocarcinoma cell line LNCaP. Endocrinology 1996; 137:4468–74.

40. van Weerden WM, Bierings HG, van Steenbrugge GJ, de Jong FH, Schroder FH. Adrenal glands of mouse and rat do not synthesize androgens. Life Sci 1992;50:857–61.

41. Keeney DS, Jenkins CM, Waterman MR. Developmentally regulated expression of adrenal 17 α-hydroxylase cytochrome P450 in the mouse embryo. Endocrinology 1995;136:4872–9.

42. Payne AH, Hales DB. Overview of steroidogenic enzymes in the pathway from cholesterol to active steroid hormones. Endocr Rev 2004;25:947–70.

43. Hu MC, Hsu HJ, Guo IC, Chung BC. Function of Cyp11a1 in animal models. Mol Cell Endocrinol 2004; 215:95–100.

44. Arakane F, Kallen CB, Watari H, et al. The mechanism of action of steroidogenic acute regulatory protein (StAR). StAR acts on the outside of mitochondria to stimulate steroidogenesis. J Biol Chem 1998;273:16339–45.

45. Acevedo HF, Goldzieher JW. The metabolism of [4-^{14}C] progesterone by hypertrophic and carcinomatous human prostate tissue. Biochim Biophys Acta 1965; 111:294–8.

46. Huang HTD. The role of the androgen receptor in prostate cancer. Crit Rev Eukaryot Gene Expr 2002;12: 193–207.